

CLIFF'S NODES

CONCERNING

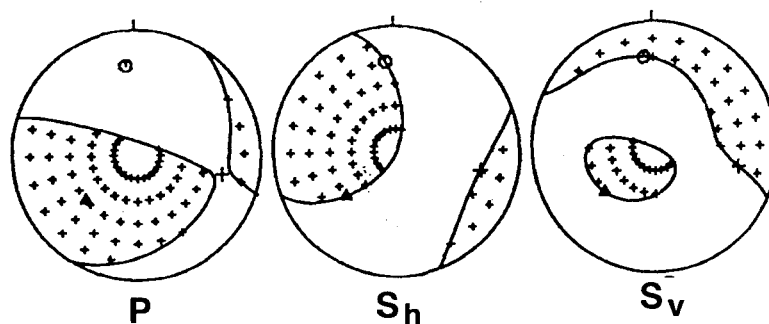
PLOTTING NODAL LINES FOR P , S_h AND S_v

BY

CLIFF FROHLICH

cliff@utig.ig.utexas.edu

ALL SAINTS DAY
1 November 1995



UNIVERSITY OF TEXAS INSTITUTE FOR GEOPHYSICS
TECHNICAL REPORT NO. 132

TABLE OF CONTENTS

Introduction	1
Brief Program Description	2
Qualitative Description of Nodal Lines for P , S_h and S_v	4
Approach	4
Nodes for P	5
Absence of Nodes for S	5
Nodes for S_h	8
Nodes for S_v	10
Derivation of Analytical Expressions for Nodal Lines.....	12
Background Concerning \mathbf{M}	12
Nodes for P	15
Absence of Nodes for S	17
Background Concerning the Earth Coordinate System	18
Nodes for S_h	19
Nodes for S_v	21
Nodes When \mathbf{M} has an Isotropic Component	21
A Note About Triangle Diagrams	23
Acknowledgments	28
References.....	28
Table 1: Principal moments and orientations of T , B , and P	30
axes for all mechanisms plotted in this report.	
To Obtain Cliff's Nodes Software From IRIS.....	31

INTRODUCTION

As earthquake seismologists, we routinely plot "beach ball" focal mechanisms describing the pattern of P -wave first-motions for ordinary, garden-variety double-couple earthquakes. But, how does one plot the pattern for S_h and S_v waves, or for earthquake sources with isotropic or compensated linear vector dipole (CLVD) components?

Recently I needed to know the answer for two reasons: to check some software I had written for constructing synthetic seismograms; and also to determine whether observations of S -waves at certain specific seismic stations had the same sign as the radiation predicted by the published Harvard centroid moment tensors (CMT). When I undertook to derive analytical expressions for the S_h and S_v nodes, I found the derivation more difficult than I had imagined. Also, in the process I learned some simple things that I should have known, but didn't (e.g., that there are no nodal lines for S , only for S_h and S_v). Thus, when I finished I resolved:

- To write down how I had determined analytical expressions for the nodal lines, because the derivations were messy enough that I was sure I would never remember if anyone asked me;
- To distribute my program to all who wanted it, so they wouldn't waste their time on such an "easy" problem;
- To ask around at the AGU meeting about who previously had written software for plotting nodal lines, as my respect for them had by now increased, whoever they were.

Thus, the purpose of this technical report is to provide background information for a Fortran program package *CliffsNodes.PShSv* for plotting focal mechanisms and nodal lines. This program package and technical report can be obtained from me via email, or from the IRIS Data Management Center (see inside back cover of this report). These efforts do not represent fundamental new research, as I have found several other people who wrote similar programs, namely Jeff Barker (see Barker, 1984), Bruce Julian (see Julian and Foulger, 1994), Thorne Lay (see Lay and Helmberger, 1983), Jose Pujol and Bob Herrmann (Pujol and Herrmann, 1990), and Terry Wallace. Interested individuals might also wish to read Kennett's (1988) suggestions for an alternative plotting strategy.

BRIEF PROGRAM DESCRIPTION

This report provides background for a Fortran program package named *CliffsNodes.PShSv*. This program package contains subroutines to plot nodal lines and focal spheres for P , S_h , and S_v energy for a moment tensor \mathbf{M} and also subroutines to plot triangle diagrams (see Figure 1). I am arranging to make this program package publicly available from the IRIS Data Management Center; it is also available from me via anonymous ftp at my email address. It is also described briefly in Frohlich (1996).

The Fortran program package itself consists of a sample main program, several user-callable subroutines for plotting focal mechanisms and triangle diagrams, and several subroutines for manipulating vectors and moment tensors. In particular, subroutines *bballP*, *bballSh*, and *bballSv* produce equal-area focal plots of nodes for P , S_h and S_v (Figure 1). The calling arguments specify azimuths, dips and principal moments for T , B , and P axes, along with the radius and center location for the focal plot. A final argument allows the user to plot "+" symbols in the positive sectors of the focal plots, if so desired. If the user does not know the azimuths, dips and principal moments for T , B , and P axes, a subroutine *TBPfind* calculates them if the user supplies the six independent elements of the moment tensor \mathbf{M} . Another subroutine, *stnPlt*, allows the user to plot symbols on the focal spheres at specified azimuths and take-off angles which, e.g., might represent seismic stations.

Similarly, a subroutine *TriDiag* plots a triangle diagram, with the calling arguments specifying the center coordinates of the plot and the base-to-vertex height of the triangle. The user can specify whether to plot lines on the triangle marking 10° intervals of dip of T , B , and P axes, or whether to plot only one line in each triangle corner containing the regions of thrust, normal faulting, and strike-slip faulting mechanisms. The user can also choose whether to plot "beach ball" icons at the edges and center of the triangle. Another subroutine *TriPlt* allows the user to plot a symbol within the diagram representing a single double-couple focal mechanism. The only necessary subroutines not provided in the package are standard plotting routines *plots*, *plot*, *newpen*, *symbol*, and *numbur*. The routine *plots* is an initialization call;

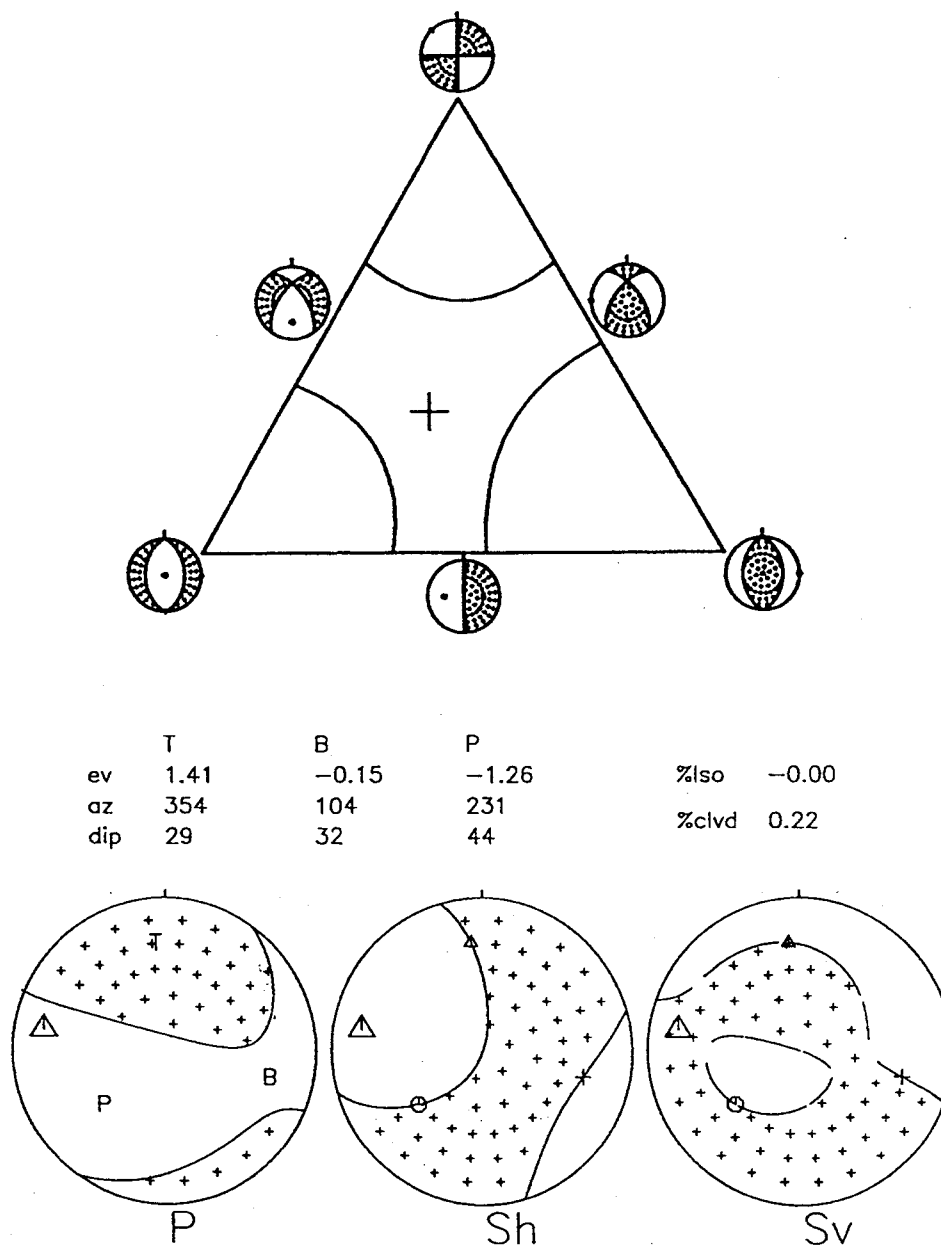


Figure 1. Plot produced by the sample program in the Fortran package *CliffsNodes.PShSv*. At the bottom of the figure are equal-area, lower hemisphere focal plots of the P , S_h , and S_v radiation pattern for the moment tensor with the T , B , and P axes and principal moments shown in the label. The program draws nodal lines, places "+" symbols in regions where the sign of the radiation is positive, and marks the position of the T , B , and P axes. Also, a large triangle marks the location of a hypothetical station, situated at azimuth of 280° E of N with a take-off-angle of 70° . In the upper part of the figure a large "+" marks where the mechanism below belongs on a triangle diagram. Note that the plotted mechanism is "regular" with respect to the rules for P , S_h , and S_v . It is "regular" for P -wave radiation because none of its principal moments are zero, and thus its two nodal lines do not intersect. It is "regular" for S_h -radiation because none of its principal axes are horizontal, and thus the two nodal lines do not intersect. It is "regular" for S_v -radiation because its B axis is not vertical, and it is not a pure double-couple with P and T axes equidistant from the vertical.

plot is a pen-command routine; *newpen* sets the pen width; *symbol* provides labels for character variables; and *numbur* provides labels for numerical information.

QUALITATIVE DESCRIPTION OF NODAL LINES FOR P , S_h , AND S_v

Approach

For an earthquake with moment tensor \mathbf{M} , I shall derive expressions for the nodal lines of P , S_h , and S_v , that is, those directions describing rays leaving the source region such that P , S_h , or S_v has zero amplitude. Note that if $\hat{\mathbf{p}}$ is a unit vector representing the direction of a ray leaving the earthquake source region, and if $\hat{\mathbf{h}}$ and $\hat{\mathbf{v}}$ are unit vectors perpendicular to one another and to $\hat{\mathbf{p}}$, with $\hat{\mathbf{h}}$ a horizontal vector, and $\hat{\mathbf{v}}$ a "vertical" vector lying in the plane formed by $\hat{\mathbf{p}}$ and the true vertical $\hat{\mathbf{z}}$ (in the earth coordinate system), then:

$$\begin{aligned} \text{amplitude } P &\sim \hat{\mathbf{p}}\mathbf{M}\hat{\mathbf{p}}^T \\ \text{amplitude } S_h &\sim \hat{\mathbf{p}}\mathbf{M}\hat{\mathbf{h}}^T \\ \text{amplitude } S_v &\sim \hat{\mathbf{p}}\mathbf{M}\hat{\mathbf{v}}^T \end{aligned} \tag{1}$$

Here $\hat{\mathbf{p}}^T$, etc. are just the transposed vectors—the column vectors corresponding to $\hat{\mathbf{p}}$, etc. Thus, the nodes for P , S_h , and S_v will occur when:

$$\bullet \text{ node } P \text{ when } 0 = \hat{\mathbf{p}}\mathbf{M}\hat{\mathbf{p}}^T \tag{2}$$

$$\bullet \text{ node } S_h \text{ when } 0 = \hat{\mathbf{p}}\mathbf{M}\hat{\mathbf{h}}^T \tag{3}$$

$$\bullet \text{ node } S_v \text{ when } 0 = \hat{\mathbf{p}}\mathbf{M}\hat{\mathbf{v}}^T \tag{4}$$

In the remainder of this section, I list a number of basic rules which qualitatively describe the nodal lines for a variety of different moment tensors, and provide examples. The objective is to provide enough examples of both "regular" and "irregular" mechanisms so that a reader could sketch the nodal lines on equal-area focal sphere plots, even when no plotting program is available.

Nodes for P

- P1: If the three principal moments of \mathbf{M} are nonzero and all have the same sign, there are no P nodes. Otherwise, there are two nodal lines, dividing the focal sphere into three zones.
- P2: The P -nodes of \mathbf{M} are fixed with respect to the T , B , and P axes, independent of rotations of \mathbf{M} .
- P3: These two nodal lines never meet and never intersect any of the three principal axes of \mathbf{M} unless one of the principal moments of \mathbf{M} is identically zero.
- P4: If one of the principal moments of \mathbf{M} is zero and the other two principal moments have opposite signs, then nodal lines fall along great circles, intersecting at the B axis.

Thus, rule P1 is that there are no P nodes if the source is implosive or explosive in all directions (Figure 2, top). Rule P3 describes the most "regular" case—when none of the three principal moments is zero but they don't all have the same sign (Figure 2, three topmost examples). Then, there are two nonintersecting nodal lines which enclose the principal axis which has the largest absolute principal moment. Rule P2 is quite useful for plotting, since in essence it states that if you can plot the P nodes in any coordinate system, you can plot them in another coordinate system just by performing a simple rotation (Figure 3). Rule P4 concerns the "irregular" case (Figure 2, bottom two examples). This actually includes most common situation for earthquake seismology—the ordinary double-couple source (Figure 2, second from bottom).

Absence of Nodes for S

- S1: The S -wave radiation pattern is independent of the isotropic component of \mathbf{M}
- S2: Unlike the case for P waves, for the full S wave there are no nodal lines,

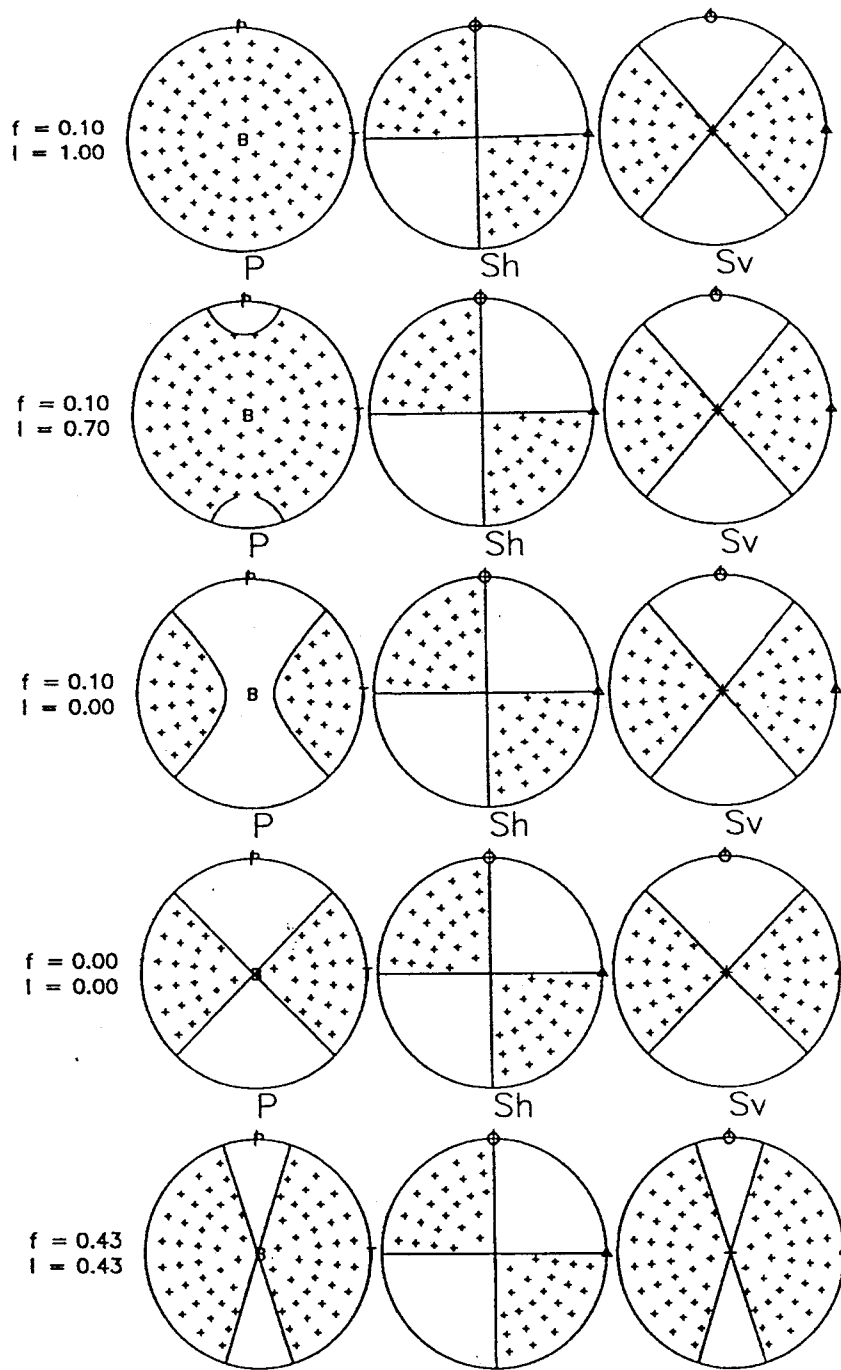


Figure 2. Sample focal plots illustrating rules P1, P3, P4, and S1 for plotting P -wave and S -wave radiation patterns. All five mechanisms have T , B , and P axes with the same orientations, only their principal moments differ from one another. All the principal moments are positive for the top mechanism, so there are no P nodes (rule P1). For the second mechanism, the P -principal moment is negative, so two nodal lines appear surrounding the P axis (P3). The third mechanism is deviatoric (i.e., has no isotropic component), but possesses a CLVD component (P3). The fourth mechanism has a pure, double-couple, strike-slip mechanism, and is "irregular" because the two nodal lines meet at the B axis (P4). The bottom mechanism is also "irregular"; it is like the second mechanism from the top but one of its principal moments is zero (P4). The top three mechanisms differ only in the amount of isotropic component—thus, they all have the same S_h and S_v radiation patterns (S1). Here the statistics f and I at left of each focal plot measure the proportions of CLVD and isotropic components as defined in equations 7 and 37.

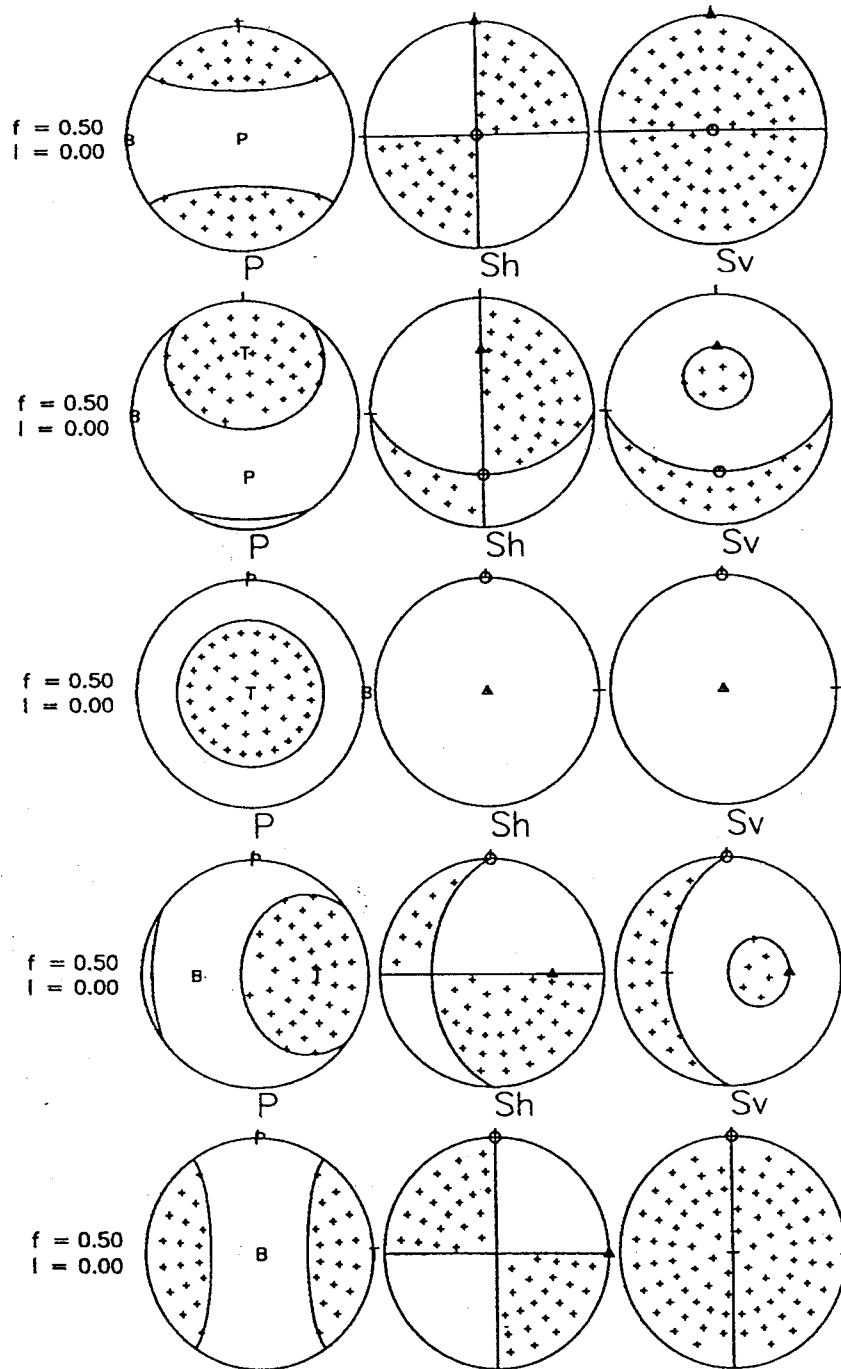


Figure 3. Sample focal plots illustrating requirements P2 and S3 for plotting P -wave and S -wave radiation patterns. All five mechanisms are pure CLVD mechanisms and thus have the same principal moments, but the orientations of their T , B , and P axes differ. The top mechanism has a polar axis oriented north-south and horizontal; the axis rotates until it reaches the vertical in the center plot; then it rotates toward the east until it becomes horizontal in the bottom plot; note that in all cases the P nodes have identical orientations with respect to the T , B , and P axes (rule P2). These mechanisms are all "irregular" with respect to their S -wave radiation pattern because they possess an S -nodal line along the equatorial axis (S3); note that this nodal line occurs for both S_h and S_v radiation.

i.e., along which $S_h^2 + S_v^2$ vanishes. Unless \mathbf{M} has a pure CLVD source this occurs only at three particular points, i.e., along the T , B , and P axes.

- S3: If \mathbf{M} has a pure CLVD source there is one equatorial nodal line; if \mathbf{M} is purely isotropic it radiates no S waves.

The first two rules are quite restrictive and quite remarkable. Basically, rule S1 asserts that there is absolutely no way of determining from S waves alone whether the source has an isotropic component (Figure 2, top three mechanisms). Rule S2 asserts that if a source is "regular" it will radiate S waves in all directions except along the three principal axes of \mathbf{M} . Rule S3 deals with two "irregular" cases (Figure 3).

Nodal lines for S_h

- S_{h1} : S_h nodes are independent of the isotropic component of \mathbf{M}
- S_{h2} : There are two S_h nodal lines, dividing the focal sphere into three zones.
- S_{h3} : The S_h -nodes are not fixed with respect to the T , B , and P axes. But, each nodal line passes through the T , B , and P axes.
 - One nodal line always passes through the P axis, the downward vertical, and the T axis in the lower hemisphere, and then the B axis in the upper hemisphere;
 - The other nodal line always passes through the T axis, the upward vertical, and the P axis in the upper hemisphere, and then the B axis in the lower hemisphere.
- S_{h4} : The two S_h -nodes never intersect unless one of the principal axes (T , B , or P) is horizontal or unless \mathbf{M} is a pure CLVD.
 - When any principal axis is horizontal, the plane perpendicular to that axis is an S_h node.

Rule S_{h2} states that, as with P , in the "regular" cases there are two non-intersecting S_h nodal lines (Figure 1; Figure 4, top three mechanisms). However rule S_{h3} states that, unlike P , they are strongly affected by rotations

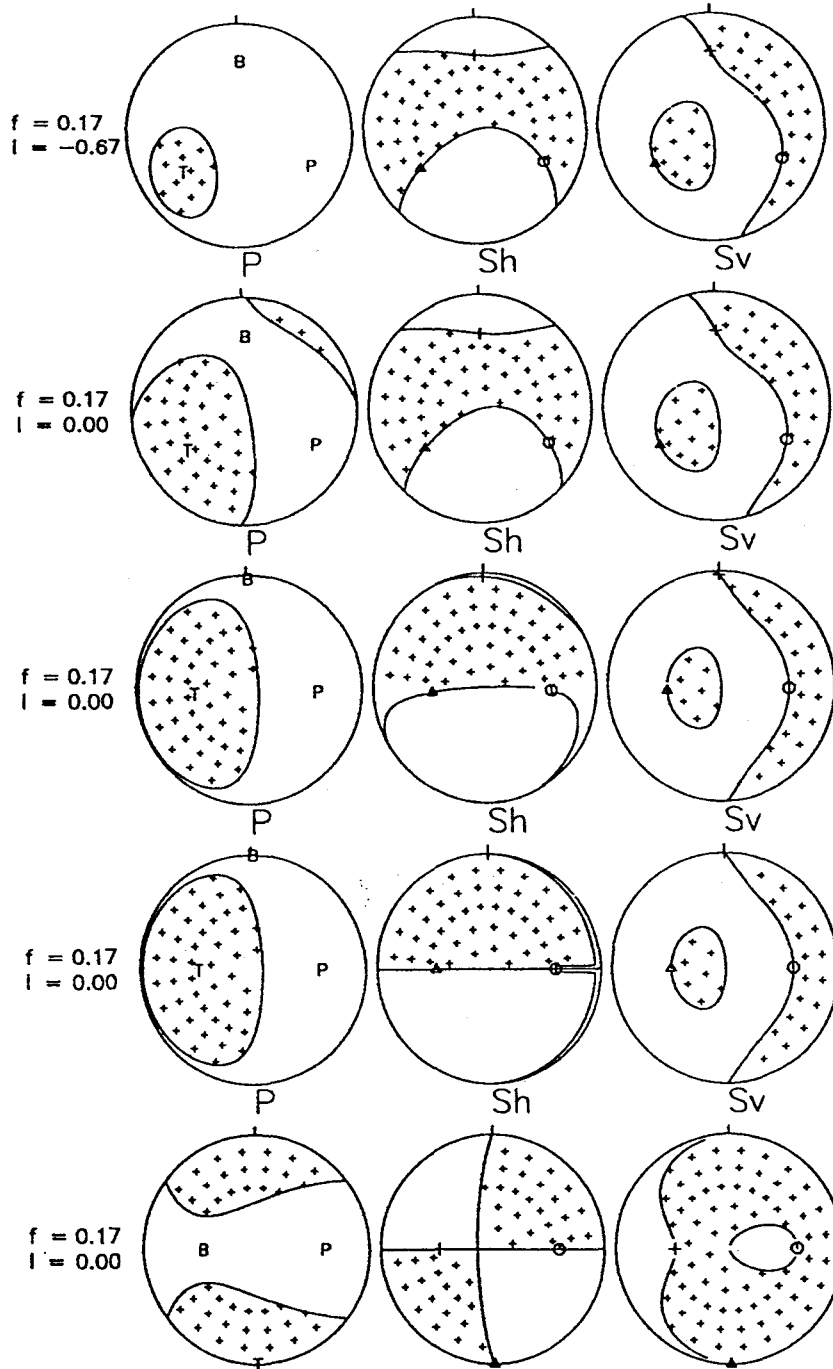


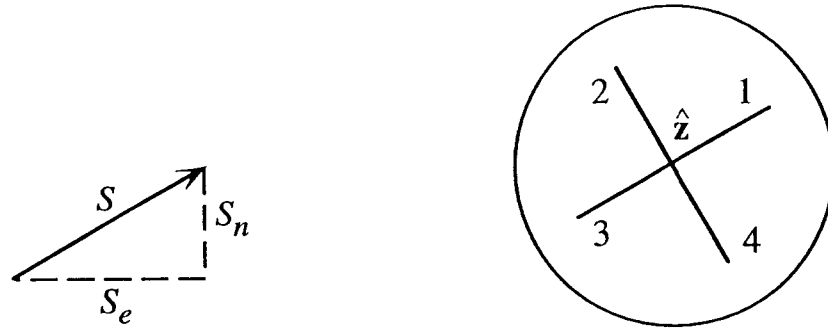
Figure 4. Sample focal plots illustrating requirements S_h1 , S_h2 , S_h3 , S_h4 , S_v1 , S_v2 and S_v3 . The top two mechanisms differ only in the amount of the isotropic component, and thus have identical S_h and S_v radiation patterns (rules S_h1 and S_v1). The top three mechanisms are all "regular" with respect to S_h , as they possess two S_h nodal lines (S_h2). All five mechanisms are "regular" with respect to S_v , as they possess three S_v nodal lines (S_v2). The bottom four mechanisms are identical except for rotation, however, note that the S_h and S_v patterns are not identical; yet, each has nodal lines passing through the vertical as well as the T , B , and P axes (S_h3 and S_v3). The bottom two mechanisms illustrate "irregular" S_h patterns, where one of the principal axes is horizontal, and so there is a vertical oriented nodal plane perpendicular to the horizontal axis (S_h4).

of \mathbf{M} . Indeed, each of the two nodal lines always passes through either the upward or downward vertical axis. This is misleading, since $\hat{\mathbf{h}}$ changes direction as we cross the vertical, and thus the vertical direction does not represent a zero in the S_h radiation pattern in the usual sense (Figure 5). In "regular" cases nodal lines also pass through the T and P axes, as well.

Rule S_h4 concerns "irregular" cases, which occur whenever one of the principal axes of \mathbf{M} is horizontal (Figure 4, bottom two mechanisms), and where there is a vertical nodal plane that is perpendicular to the horizontal axis. For sketching nodes, it is useful to remember that when any principal axis is nearly horizontal, the nodal lines will closely approach the associated perpendicular vertical plane (Figure 4, third and fourth mechanism).

Nodes for S_v

- S_v1 : S_v nodes are independent of the isotropic component of \mathbf{M}
- S_v2 : There are three S_v nodal lines, dividing the focal sphere into four zones.
- S_v3 : The S_v -nodes are not fixed with respect to the T , B , and P axes.
 - But, one nodal line (usually roughly circular or oblong in shape) passes through the upward vertical and the either the T or P axis, depending on which is closer to the vertical.
 - A second nodal line of the same shape passes through the downward vertical and either the T or P axis, depending on which is closer to the vertical.
 - A third nodal lines passes through the B axis and either the T or P axis, depending on which is closer to the horizontal.
- S_v4 : The nodal lines only intersect in certain special cases:
 - If the B axis is vertical (or, \mathbf{M} is a pure CLVD and the plane of symmetry passes through the vertical),
 - If \mathbf{M} is a pure double couple and the T and P axes are equidistant from the vertical.



	1	2	3	4
$\hat{\mathbf{h}}_e$				
$\hat{\mathbf{v}}_e$				
S_h	0	-	0	+
S_v	-	0	+	0

Figure 5. The nodal lines for S_h and S_v cross the vertical in all cases, but the vertical direction does not represent a zero in the radiation pattern in the usual sense. When none of the three principal axes of \mathbf{M} coincide with the vertical $\hat{\mathbf{z}}$, then there will be an S wave, with north-south and east-west components given by $S_n = \hat{\mathbf{z}}\mathbf{M}\hat{\mathbf{n}}^T$ and $S_e = \hat{\mathbf{z}}\mathbf{M}\hat{\mathbf{e}}^T$, respectively (top left). On a blowup of the near-vertical region of the focal sphere (top right), as we cross the vertical along a line parallel to the direction of S (line 1-3) there will be a nodal line for S_h . Yet, along a line perpendicular to the direction of S (line 2-4 at top right), S_h changes from large and negative to large and positive because the direction of $\hat{\mathbf{h}}$ changes as we cross the vertical. Similarly, there is a nodal line for S_v along a line perpendicular to S (line 2-4), while S_v changes from large and negative to large and positive as we cross vertical along the parallel direction (line 1-3) because the direction of $\hat{\mathbf{v}}$ changes.

Rule S_v2 states that, unlike P and S_h , in the "regular" cases there are three non-intersecting S_v nodal lines (Figure 4). However rule S_v3 states that, unlike P and like S_h , they are strongly affected by rotations of \mathbf{M} . Indeed, two of the nodal lines always pass through either the upward or downward vertical axis. This is misleading, since \hat{v} changes direction as we cross the vertical, and thus the vertical direction does not represent a zero in the S_v radiation pattern in the usual sense (Figure 5). In "regular" cases these two nodal lines also pass through either the T or the P axis, whichever is closer to the vertical; while the third nodal line passes through the B axis and either the T or P axis, whichever remains (Figure 4). Rule S_v4 concerns "irregular" cases, which occur whenever the B axis is vertical, or, when \mathbf{M} is a double-couple and the T and P axes are equidistant from the vertical (Figure 6).

DERIVATION OF ANALYTICAL EXPRESSIONS FOR NODAL LINES

Background Concerning \mathbf{M}

For convenience, assume that we know all the information about \mathbf{M} that is routinely provided in the Harvard CMT catalog, i.e., the values for the six independent elements m_{ij} of \mathbf{M} as well as the dips ($\alpha_T, \alpha_B, \alpha_P$), strikes (ϕ_T, ϕ_B, ϕ_P), and principal eigenvalues ($\lambda_T, \lambda_B, \lambda_P$) of the T , B , and P axes of \mathbf{M} . In particular:

$$\mathbf{M} = \begin{bmatrix} m_{11} & m_{12} & m_{13} \\ m_{12} & m_{22} & m_{23} \\ m_{13} & m_{23} & m_{33} \end{bmatrix} = \mathbf{R} \begin{bmatrix} \lambda_T & 0 & 0 \\ 0 & \lambda_B & 0 \\ 0 & 0 & \lambda_P \end{bmatrix} \mathbf{R}^T \quad (5)$$

where \mathbf{R} is an (unspecified) rotation matrix which brings vectors described in the principal axis system to the usual earth coordinate system, and \mathbf{R}^T is the transpose of \mathbf{R} . In the earth coordinate system, the unit vectors \hat{a}_T , \hat{a}_B , and \hat{a}_P describing the three principal axes are:

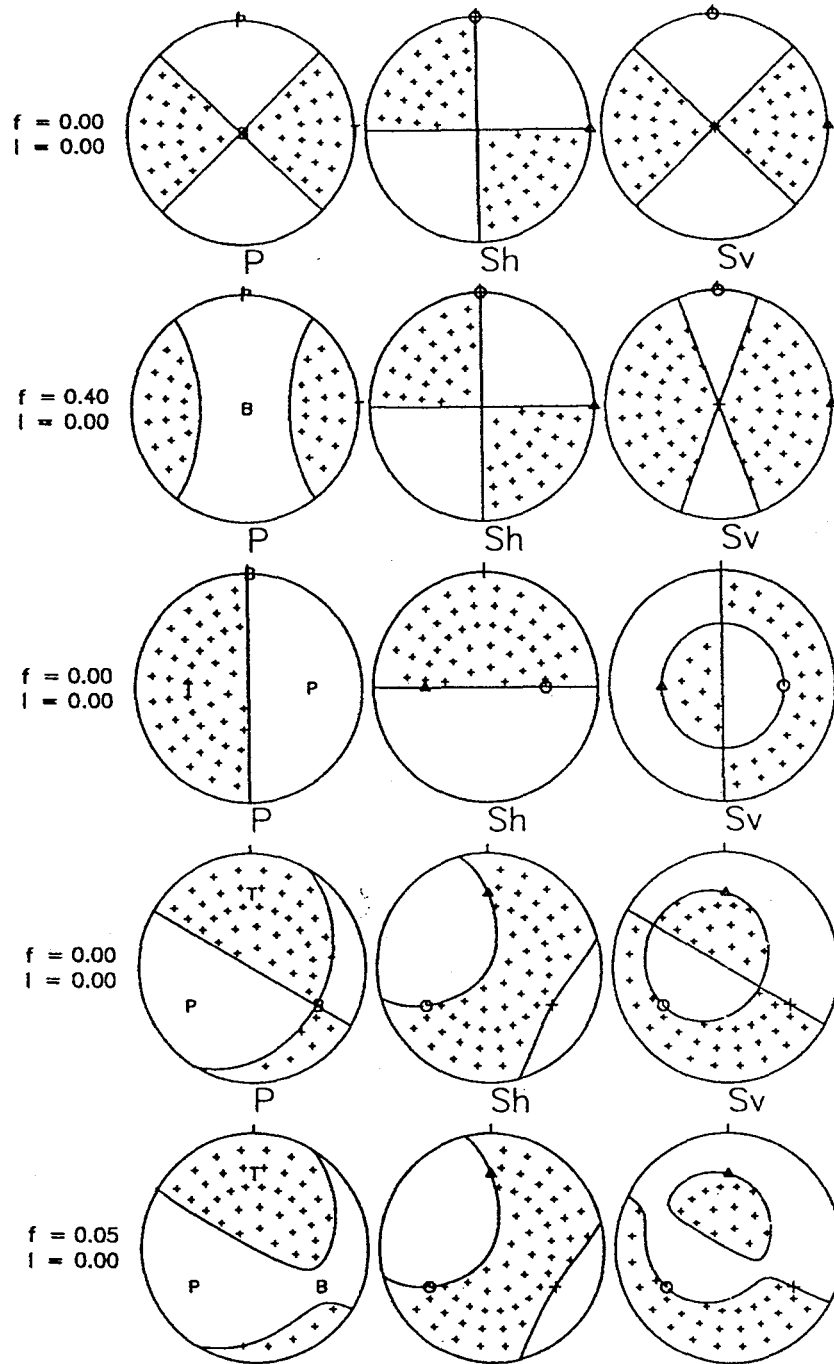


Figure 6. Sample focal plots illustrating rule S_v4 . The top four plots are "irregular" in that the nodal lines for S_v intersect one another. In the top two mechanisms this occurs because the B axis is vertical; the third and fourth mechanisms are pure double couples with the P and T axes equidistant from the vertical. The bottom two mechanisms are identical except that the bottom mechanism has a small CLVD component.

$$\begin{aligned}
\hat{\mathbf{a}}_T &= (-\sin \alpha_T, \cos \alpha_T \sin \phi_T, \cos \alpha_T \cos \phi_T) \\
\hat{\mathbf{a}}_B &= (-\sin \alpha_B, \cos \alpha_B \sin \phi_B, \cos \alpha_B \cos \phi_B) \\
\hat{\mathbf{a}}_P &= (-\sin \alpha_P, \cos \alpha_P \sin \phi_P, \cos \alpha_P \cos \phi_P)
\end{aligned} \tag{6}$$

For now we assume that \mathbf{M} is deviatoric (i.e., that $\lambda_T + \lambda_B + \lambda_P = 0$), although we shall relax this condition later. For later computational convenience we rewrite \mathbf{M} to show explicitly the dependence on f , the strength of the non-double-couple component.

$$\mathbf{R}^T \mathbf{M} \mathbf{R} = \begin{bmatrix} \lambda_T & 0 & 0 \\ 0 & \lambda_B & 0 \\ 0 & 0 & \lambda_P \end{bmatrix} = \lambda_T \begin{bmatrix} 1 & 0 & 0 \\ 0 & -f & 0 \\ 0 & 0 & -1+f \end{bmatrix} \text{ or } \lambda_P \begin{bmatrix} -1+f & 0 & 0 \\ 0 & -f & 0 \\ 0 & 0 & 1 \end{bmatrix} \tag{7}$$

where $f = \frac{-\lambda_B}{\lambda_T}$ if $|\lambda_T| > |\lambda_P|$ and \mathbf{M} represents a mechanism of the polar T type, and $f = -\frac{\lambda_B}{\lambda_P}$ if $|\lambda_P| > |\lambda_T|$ and \mathbf{M} is of the polar P type.

Since in both cases the relative sizes of P , S_h and S_v waves depend entirely on the relative sizes of the diagonal terms (1, $-f$, and $-1+f$), there is no loss of generality if we perform all subsequent calculations in the principal axis system and use instead of \mathbf{M} the "reduced" moment tensor \mathbf{M}_R

$$\mathbf{M}_R = \begin{bmatrix} 1 & 0 & 0 \\ 0 & -f & 0 \\ 0 & 0 & -1+f \end{bmatrix} \tag{8}$$

where the 1 axis is the "dominant" or D axis (T if $|\lambda_T| > |\lambda_P|$; P if $|\lambda_P| > |\lambda_T|$), the 2 axis is the B axis, and the 3 axis is the "minor" or M axis (P if $|\lambda_T| > |\lambda_P|$; T if $|\lambda_P| > |\lambda_T|$).

Nodes for P

For a ray leaving the source region in the direction along unit direction vector $\hat{\mathbf{p}}$, the strength of the P wave is proportional to $\hat{\mathbf{p}}\mathbf{M}_R\hat{\mathbf{p}}^T$. In the DBM coordinate system (see Figure 7) the explicit expressions for $\hat{\mathbf{p}}$, $\hat{\mathbf{p}}\mathbf{M}_R$, and $\hat{\mathbf{p}}\mathbf{M}_R\hat{\mathbf{p}}^T$ are:

$$\hat{\mathbf{p}} = (\cos \alpha, \sin \alpha \sin \phi, \sin \alpha \cos \phi) \quad (9)$$

where α is the angle between $\hat{\mathbf{p}}$ and the D axis, and ϕ is the azimuthal angle, the angle with respect to the M axis of the projection of $\hat{\mathbf{p}}$ in the B-M plane.

$$\hat{\mathbf{p}}\mathbf{M}_R = (\cos \alpha, -f \sin \alpha \sin \phi, (-1+f) \sin \alpha \cos \phi) \quad (10)$$

$$\hat{\mathbf{p}}\mathbf{M}_R\hat{\mathbf{p}}^T = \cos^2 \alpha - \sin^2 \alpha \left[\frac{1}{2} + \left(\frac{1}{2} - f \right) \cos 2\phi \right] \quad (11)$$

Now, $\hat{\mathbf{p}}$ lies on a node for P when $\hat{\mathbf{p}}\mathbf{M}_R\hat{\mathbf{p}}^T$ vanishes, which occurs whenever:

$$\sin^2 \alpha_N = \frac{2}{3 + (1 - 2f) \cos 2\phi} \quad (12)$$

There are two nodal lines, since if (α_N, ϕ) lie on a nodal line, then $(180^\circ - \alpha_N, \phi)$ also lie along a nodal line.

Thus, to plot nodes for P we allow ϕ to vary from 0° to 360° , and use eq. (12) to determine the angle α_N where the node occurs. We then plot this on a focal sphere in the earth coordinate system using eq. (9) and eq. (6) above.

$$\hat{\mathbf{P}}_N = \cos \alpha_N \hat{\mathbf{a}}_T + \sin \alpha_N \sin \phi \hat{\mathbf{a}}_B + \sin \alpha_N \cos \phi \hat{\mathbf{a}}_P \quad (13)$$

Note that for any direction $\hat{\mathbf{p}}$ in space, $\hat{\mathbf{p}}\mathbf{M}_R\hat{\mathbf{p}}^T$ is independent of the coordinate system chosen to represent $\hat{\mathbf{p}}$ and \mathbf{M}_R , thus the nodes of P always have the same geometric relationship to the T , B , and P axes $\hat{\mathbf{a}}_T$, $\hat{\mathbf{a}}_B$, and $\hat{\mathbf{a}}_P$.

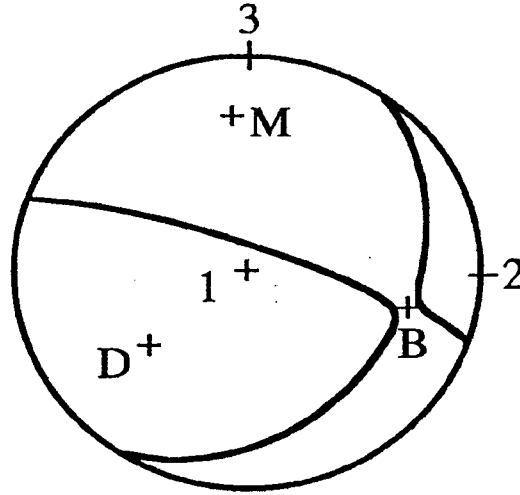


Figure 7. The two coordinate systems used in derivations in this report. In the "earth system" the three coordinate axes are vertical downward (labeled "1"), horizontal due east (labeled "2"), and horizontal due north (labeled "3"). In the "DBM" system the three coordinate axes coincide with the T (D), B , and P (M) axes of the focal mechanism.

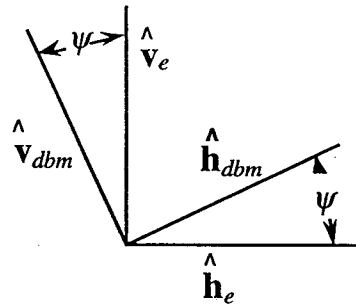


Figure 8. At any point \hat{p} on the focal sphere, there is a rotation angle ψ which brings the orientations of the horizontal and vertical directions in the earth system (\hat{h}_e and \hat{v}_e) in correspondence with the horizontal and vertical directions (\hat{h}_{dbm} , and \hat{v}_{dbm}), in the principal axis or DBM system.

Absence of Nodes for S

Do there exist directions leaving the source for which the full S wave vanishes? To answer this we evaluate the reduced amplitudes of S in the DBM system. In particular, for a ray leaving along direction $\hat{\mathbf{p}}$ (see eq. (9)), in the DBM system a horizontal direction vector $\hat{\mathbf{h}}_{dbm}$ and a vertical direction vector $\hat{\mathbf{v}}_{dbm}$ are:

$$\hat{\mathbf{h}}_{dbm} = (0, -\cos \phi, \sin \phi) \quad (14)$$

$$\hat{\mathbf{v}}_{dbm} = (-\sin \alpha, \cos \alpha \sin \phi, \cos \alpha \cos \phi) \quad (15)$$

Thus, the reduced amplitudes of the components of the S wave along these directions are:

$$\hat{\mathbf{p}}\mathbf{M}\mathbf{R}\hat{\mathbf{h}}_{dbm}^T = \sin \alpha \sin 2\phi \left(-\frac{1}{2} + f \right) \quad (16)$$

$$\hat{\mathbf{p}}\mathbf{M}\mathbf{R}\hat{\mathbf{v}}_{dbm}^T = -\sin \alpha \cos \alpha \left[\frac{3}{2} + \left(\frac{1}{2} - f \right) \cos 2\phi \right] \quad (17)$$

The full S wave will vanish if $(\hat{\mathbf{p}}\mathbf{M}\mathbf{R}\hat{\mathbf{h}}_{dbm}^T)^2 + (\hat{\mathbf{p}}\mathbf{M}\mathbf{R}\hat{\mathbf{v}}_{dbm}^T)^2$ is zero.

$$0 = \sin^2 \alpha \left[[\sin 2\phi(1-2f)]^2 + [\cos \alpha [3 + (1-2f)\cos 2\phi]]^2 \right] \quad (18)$$

Inspection shows that this occurs generally only in three special cases. These are:

- $\alpha = 0^\circ$ – this corresponds to the D axis
- $\alpha = 90^\circ$ and $\phi = 0^\circ$ – this corresponds to the M axis
- $\alpha = 90^\circ$ and $\phi = 90^\circ$ – this corresponds to the B axis

Thus, we have shown that the full S wave vanishes only along the T , B , and P axes; there are no nodal lines for S in the sense that they exist for P . Also, if $f = 0.5$, there will be a nodal line where $\alpha = 90^\circ$.

Background Concerning the Earth Coordinate System

While eqs. (16) and (17) represent S_h and S_v amplitudes in the DBM coordinate system, these are not usually equivalent to S_h and S_v as observed by a seismologist since in the earth system the horizontal and vertical unit vectors $\hat{\mathbf{h}}_e$ and $\hat{\mathbf{v}}_e$ are not the same as $\hat{\mathbf{h}}_{dbm}$ and $\hat{\mathbf{v}}_{dbm}$ in the DBM system. However, all four vectors $\hat{\mathbf{h}}_e$, $\hat{\mathbf{v}}_e$, $\hat{\mathbf{h}}_{dbm}$, and $\hat{\mathbf{v}}_{dbm}$ represent the directions of S waves and thus lie in a plane perpendicular to $\hat{\mathbf{p}}$; also, there must exist some rotation angle ψ so that perpendicular vectors $\hat{\mathbf{h}}_e$ and $\hat{\mathbf{v}}_e$ are simply the rotation of $\hat{\mathbf{h}}_{dbm}$ and $\hat{\mathbf{v}}_{dbm}$ by ψ about $\hat{\mathbf{p}}$ (Figure 8). Thus, in the earth system we can determine the amplitudes of S_h and S_v by a simple rotation:

$$S_h \text{ amplitude} \sim \hat{\mathbf{p}}\mathbf{M}\mathbf{R}\hat{\mathbf{h}}_e^T = \hat{\mathbf{p}}\mathbf{M}\mathbf{R}\hat{\mathbf{h}}_{dbm}^T \cos \psi + \hat{\mathbf{p}}\mathbf{M}\mathbf{R}\hat{\mathbf{v}}_{dbm}^T \sin \psi \quad (19)$$

$$S_v \text{ amplitude} \sim \hat{\mathbf{p}}\mathbf{M}\mathbf{R}\hat{\mathbf{v}}_e^T = -\hat{\mathbf{p}}\mathbf{M}\mathbf{R}\hat{\mathbf{h}}_{dbm}^T \sin \psi + \hat{\mathbf{p}}\mathbf{M}\mathbf{R}\hat{\mathbf{v}}_{dbm}^T \cos \psi \quad (20)$$

To find the nodes, we set these expressions to zero and (unless $\psi = 0^\circ$ or $\psi = 90^\circ$) solve to find:

$$\text{For } S_h: \cos \alpha_N = \frac{-\cot \psi (1-2f) \sin 2\phi}{3 + (1-2f) \cos 2\phi} \quad (21)$$

$$\text{For } S_v: \cos \alpha_N = \frac{+\tan \psi (1-2f) \sin 2\phi}{3 + (1-2f) \cos 2\phi} \quad (22)$$

But, what is the angle ψ ? Note that $\hat{\mathbf{h}}_{dbm} \cdot \hat{\mathbf{v}}_e = \sin \psi$ and $\hat{\mathbf{h}}_{dbm} \cdot \hat{\mathbf{h}}_e = \cos \psi$ (see Figure 8), so that:

$$\tan \psi = \frac{\hat{\mathbf{h}}_{dbm} \cdot \hat{\mathbf{v}}_e}{\hat{\mathbf{h}}_{dbm} \cdot \hat{\mathbf{h}}_e} \quad (23)$$

Suppose that in the DBM system the vector $\hat{\mathbf{z}}$ which represents the vertical in the earth system has dip and azimuth a and t , i. e.:

$$\hat{\mathbf{z}} = (\cos a, \sin a \sin t, \sin a \cos t) \quad (24)$$

Now, by the rules of cross products, $(\hat{\mathbf{z}} \times \hat{\mathbf{p}})$ is a vector parallel to $\hat{\mathbf{h}}_e$, with length equal to the sine of the angle between $\hat{\mathbf{z}}$ and $\hat{\mathbf{p}}$; furthermore, $\hat{\mathbf{p}} \times (\hat{\mathbf{z}} \times \hat{\mathbf{p}})$ is a vector parallel to $\hat{\mathbf{v}}_e$, also with the same length as $(\hat{\mathbf{z}} \times \hat{\mathbf{p}})$. Thus

$$\tan \psi = \frac{\hat{\mathbf{h}}_{dbm} \cdot (\hat{\mathbf{p}} \times (\hat{\mathbf{z}} \times \hat{\mathbf{p}}))}{\hat{\mathbf{h}}_{dbm} \cdot (\hat{\mathbf{z}} \times \hat{\mathbf{p}})} = \frac{\hat{\mathbf{h}}_{dbm} \cdot \hat{\mathbf{z}} - (\hat{\mathbf{h}}_{dbm} \cdot \hat{\mathbf{p}})(\hat{\mathbf{p}} \cdot \hat{\mathbf{z}})}{\det \begin{bmatrix} \hat{\mathbf{h}}_{dbm} \\ \hat{\mathbf{p}} \\ \hat{\mathbf{z}} \end{bmatrix}} = \frac{\hat{\mathbf{z}} \cdot \hat{\mathbf{h}}_{dbm}}{\det \begin{bmatrix} \hat{\mathbf{h}}_{dbm} \\ \hat{\mathbf{p}} \\ \hat{\mathbf{z}} \end{bmatrix}} \quad (25)$$

Here, we have used the fact that $\hat{\mathbf{h}}_{dbm} \cdot \hat{\mathbf{p}} = 0$ and the vector identities:

$$\bar{\mathbf{A}} \times (\bar{\mathbf{B}} \times \bar{\mathbf{C}}) = \bar{\mathbf{B}}(\bar{\mathbf{A}} \cdot \bar{\mathbf{C}}) - \bar{\mathbf{C}}(\bar{\mathbf{A}} \cdot \bar{\mathbf{B}}) \quad (26)$$

$$\bar{\mathbf{A}} \cdot (\bar{\mathbf{B}} \times \bar{\mathbf{C}}) = \det \begin{bmatrix} \bar{\mathbf{A}} \\ \bar{\mathbf{B}} \\ \bar{\mathbf{C}} \end{bmatrix} = \det \begin{bmatrix} a_1 & a_2 & a_3 \\ b_1 & b_2 & b_3 \\ c_1 & c_2 & c_3 \end{bmatrix}$$

which hold for any three vectors, $\bar{\mathbf{A}} = (a_1, a_2, a_3)$, $\bar{\mathbf{B}} = (b_1, b_2, b_3)$, and $\bar{\mathbf{C}} = (c_1, c_2, c_3)$. Evaluating eq. 25 using the explicit representations for $\hat{\mathbf{h}}_{dbm}$ (eq. 14), $\hat{\mathbf{p}}$ (eq. 9), and $\hat{\mathbf{z}}$ (eq. 24), we find:

$$\tan \psi = \frac{\sin a \sin(\phi - t)}{\sin \alpha \cos a - \cos \alpha \sin a \cos(\phi - t)} \quad (27)$$

Nodes for S_h

If we combine eqs. 21 and 27, we obtain:

$$\cos \alpha_N = \frac{-[\sin \alpha_N \cos a - \cos \alpha_N \sin a \cos(\phi - t)](1 - 2f) \sin 2\phi}{\sin a \sin(\phi - t)(3 + (1 - 2f) \cos 2\phi)} \quad (28)$$

If $f \neq 0.5$, $a \neq 0$, and $a \neq 90^\circ$, then we can solve this explicitly for $\tan \alpha_N$, i.e.:

$$\tan \alpha_N = \tan a \left[-\frac{(3 + (1 - 2f) \cos 2\phi) \sin(\phi - t)}{\sin 2\phi(1 - 2f)} + \cos(\phi - t) \right] \quad (29)$$

Note that the nodal lines described by eq. (29) passes through all three principal axes of **M**. The quantity on the right in brackets becomes infinite, and thus $\alpha_N = 90^\circ$ when ϕ approaches either 0° or 90° , thus showing that the *B* and *M* axes, respectively, lie along the nodal line. It is not difficult to show that the quantity in brackets must also vanish for some value of ϕ , so that the *D* axis lies along the nodal line as well.

In the special case when $f = 0.5$, then, $\cos \alpha_N = 0$, and there will be a nodal line for $\alpha_N = 90^\circ$ (i.e., along the *B-M* plane). Also, if $a = 90^\circ$, then $\cos \alpha_N$ factors out of both sides of eq. (28), and we are left with a node for all α_N when ϕ satisfies:

$$\tan(\phi - t) = \frac{(1 - 2f) \sin 2\phi}{3 + (1 - 2f) \cos 2\phi} \quad (30)$$

In either case, we can use eq. (13) to plot the nodal lines explicitly.

In practice, it is useful to note that whenever either the *D* axis, the *B* axis, or the *M* axis is horizontal, then the corresponding perpendicular vertical plane will be a nodal plane. This includes the case above where $a = 0$, since then both *B* and *M* are horizontal, and both lie within vertical nodal planes.

The only missing detail is that angles a and t which describe $\hat{\mathbf{z}}$ in DBM coordinates are not given explicitly in the Harvard CMT catalog. However, it is straightforward to show that if the *T* axis is the dominant axis then:

$$\begin{aligned} a &= 90^\circ - \alpha_T \\ \tan t &= \frac{\sin \alpha_B}{\sin \alpha_P} \end{aligned} \quad (31)$$

while if the P axis is the dominant axis then:

$$\begin{aligned} a &= 90^\circ - \alpha_P \\ \tan t &= \frac{\sin \alpha_B}{\sin \alpha_T} \end{aligned} \quad (32)$$

Nodes for S_v

Combining eqs. (22) and (27) we obtain:

$$\cos \alpha_N = \frac{\sin a \sin(\phi - t)(1 - 2f) \sin 2\phi}{[\sin \alpha_N \cos a - \cos \alpha_N \sin a \cos(\phi - t)](3 + \cos 2\phi(1 - 2f))} \quad (33)$$

As with the S_h case, if $f = 0.5$ (or if $a = 0$) there will be a node for $\alpha_N = 90^\circ$. Otherwise, after some manipulation one obtains a quadratic equation in $\tan \alpha_N$:

$$\begin{aligned} 0 &= \tan^2 \alpha_N + \tan \alpha_N \left[\frac{3 + \cos 2\phi(2f - 1)}{\tan a \sin(\phi - t) \sin 2\phi(1 - 2f)} \right] \\ &\quad + 1 + \frac{[3 + \cos 2\phi(1 - 2f)] \cos(\phi - t)}{\sin 2\phi \sin(\phi - t)(1 - 2f)} \end{aligned} \quad (34)$$

For plotting the nodes of S_v , one simply solves eq. (34) using the binomial theorem, and plots the nodes using eq. (13).

Note that unlike the nodes of P , the nodes of S_v and S_h depend on the relationship between the vertical $\hat{\mathbf{z}}$ and the position of the D axis. This is because $\hat{\mathbf{h}}_e$ and $\hat{\mathbf{v}}_e$ depend on $\hat{\mathbf{z}}$, and thus so do $\hat{\mathbf{p}}\mathbf{M}\mathbf{R}\hat{\mathbf{h}}_e^T$ and $\hat{\mathbf{p}}\mathbf{M}\mathbf{R}\hat{\mathbf{v}}_e^T$. Thus, unlike the P situation, it is not possible to determine S_h and S_v nodes by simply rotating the nodes determined for any particular coordinate system, such as the DBM system.

Nodes When \mathbf{M} has an Isotropic Component

If \mathbf{M} has an isotropic component it is possible to rewrite \mathbf{M} as the sum of a pure isotropic tensor \mathbf{M}_I and a deviatoric tensor \mathbf{M}_D , i.e., $\mathbf{M} = \mathbf{M}_I + \mathbf{M}_D$. Following eq. (7), in DBM coordinates this would be:

$$\mathbf{R}^T \mathbf{M} \mathbf{R} = \lambda_I \begin{bmatrix} 1 & 0 & 0 \\ 0 & 1 & 0 \\ 0 & 0 & 1 \end{bmatrix} + \lambda_D \begin{bmatrix} 1 & 0 & 0 \\ 0 & -f & 0 \\ 0 & 0 & -1+f \end{bmatrix} \quad (35)$$

where $\lambda_D = \lambda_T$ or $\lambda_D = \lambda_P$, depending on whether T or P is the dominant axis of \mathbf{M}_D .

The amplitudes of P , S_h and S_v waves (eq. (1)) are:

$$\begin{aligned} \text{amplitude } P &\sim \hat{\mathbf{p}} \mathbf{M} \hat{\mathbf{p}}^T = \hat{\mathbf{p}} \mathbf{M}_I \hat{\mathbf{p}}^T + \hat{\mathbf{p}} \mathbf{M}_D \hat{\mathbf{p}}^T \\ \text{amplitude } S_h &\sim \hat{\mathbf{p}} \mathbf{M} \hat{\mathbf{h}}_e^T = \hat{\mathbf{p}} \mathbf{M}_I \hat{\mathbf{h}}_e^T + \hat{\mathbf{p}} \mathbf{M}_D \hat{\mathbf{h}}_e^T = \hat{\mathbf{p}} \mathbf{M}_D \hat{\mathbf{h}}_e^T \\ \text{amplitude } S_v &\sim \hat{\mathbf{p}} \mathbf{M} \hat{\mathbf{v}}_e^T = \hat{\mathbf{p}} \mathbf{M}_I \hat{\mathbf{v}}_e^T + \hat{\mathbf{p}} \mathbf{M}_D \hat{\mathbf{v}}_e^T = \hat{\mathbf{p}} \mathbf{M}_D \hat{\mathbf{v}}_e^T \end{aligned} \quad (36)$$

Since the amplitudes for S_h and S_v depend only on the deviatoric part of tensor, their nodes are exactly as we have derived previously unless $\mathbf{M}_D = 0$, in which case there will be no S waves in any direction.

For P waves, we can construct a "reduced" moment tensor equivalent to eq. (8):

$$\mathbf{M}_R = \begin{bmatrix} 1+I & 0 & 0 \\ 0 & -f+I & 0 \\ 0 & 0 & -1+f+I \end{bmatrix} \quad (37)$$

where the parameter $I = \frac{\lambda_I}{\lambda_D}$.

The amplitude of P depends on I :

$$\hat{\mathbf{p}}\mathbf{M}_R\hat{\mathbf{p}}^T = \mathbf{I} + \cos^2 \alpha - \sin^2 \alpha \left[\frac{1}{2} + \left(\frac{1}{2} - f \right) \cos 2\phi \right] \quad (38)$$

and the P amplitude vanishes when:

$$\sin^2 \alpha_N = \frac{2 + 2I}{3 + (1 - 2f)\cos 2\phi} \quad (39)$$

This is a straightforward extension of eq. (12), so that it is possible to plot the P nodes using eq. (13). Note that unless the strength I lies in the range between -1 and $1-f$ there will be no P nodes whatsoever.

A NOTE ABOUT TRIANGLE DIAGRAMS

Triangle diagrams (Figure 1 and Figure 9) are a quantitative graphical scheme for displaying information about the dip angles of one or more double-couple focal mechanisms. On the triangle diagram each mechanism is plotted as a single point; pure thrust mechanisms, pure normal faulting mechanisms, and pure strike-slip mechanisms each plot in their respective corners of the triangle, while mechanisms with a component of all three types of faulting plot in the interior. As demonstrated in Frohlich (1992) and Frohlich and Apperson (1992), they are especially useful if one requires a display which illustrates the amount of similarity or dissimilarity among a large number of double-couple mechanisms.

The purpose of this note is to describe triangle diagrams, as a subroutine *TriDiag* for plotting them is included in the *CliffsNodes* software package. In addition I wish to correct an error in the previously published equations for plotting the triangle diagrams. This error appears in the equations (but not in the figures) which appear in both Frohlich (1992) and Frohlich and Apperson (1992).

It is possible to plot a double-couple focal mechanism as a unique point on a triangle diagram because the T , B and P axes are mutually perpendicular. Thus, if α_T , α_B , and α_P are the dips angles of the T , B and P axes, respectively, then:

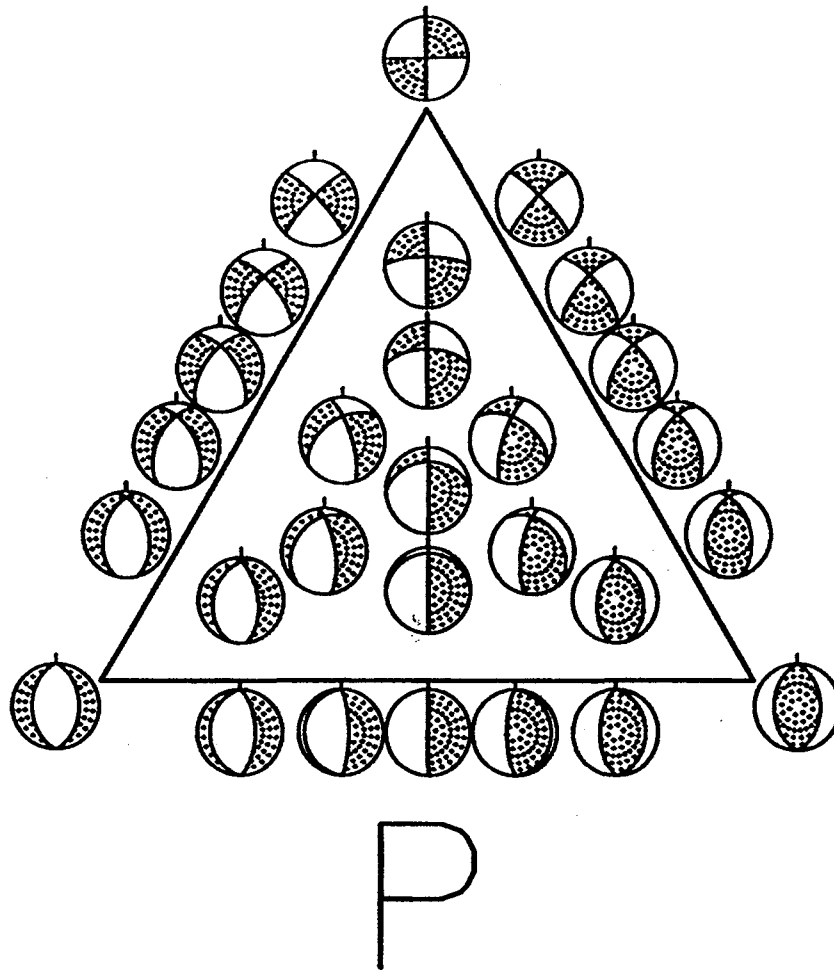
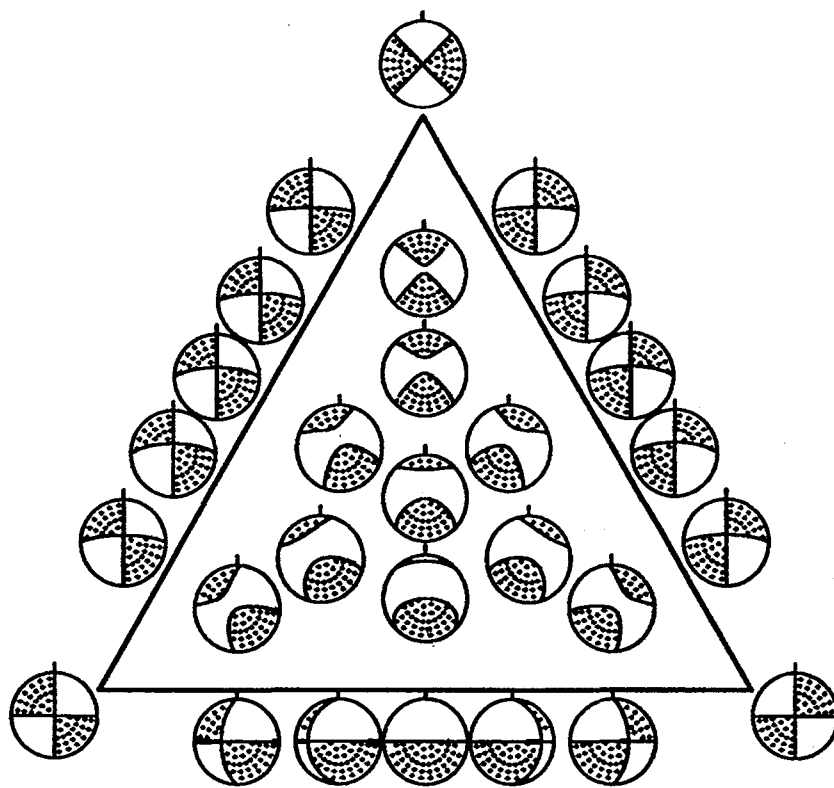


Figure 9a

Figure 9. Triangle diagrams with P (Figure 9a), S_h (Figure 9b) and S_v (Figure 9c) radiation patterns for 28 double-couple mechanisms, chosen to illustrate the range of possible types. For the seven focal plots along each edge of the triangle, one principal axis is horizontal (B horizontal along bottom edge; P along right edge; T along left edge), and the other two axes dip at angles of 0° , 15° , 30° , 45° , 60° , 75° and 90° with respect to the horizontal. For each focal plot in the triangle interior, two axes have identical dip angles (thus plotting along lines bisecting the angles and sides) while the third axis makes angles of 15° , 35.3° , 60° and 75° with the horizontal.



Sh

Figure 9b

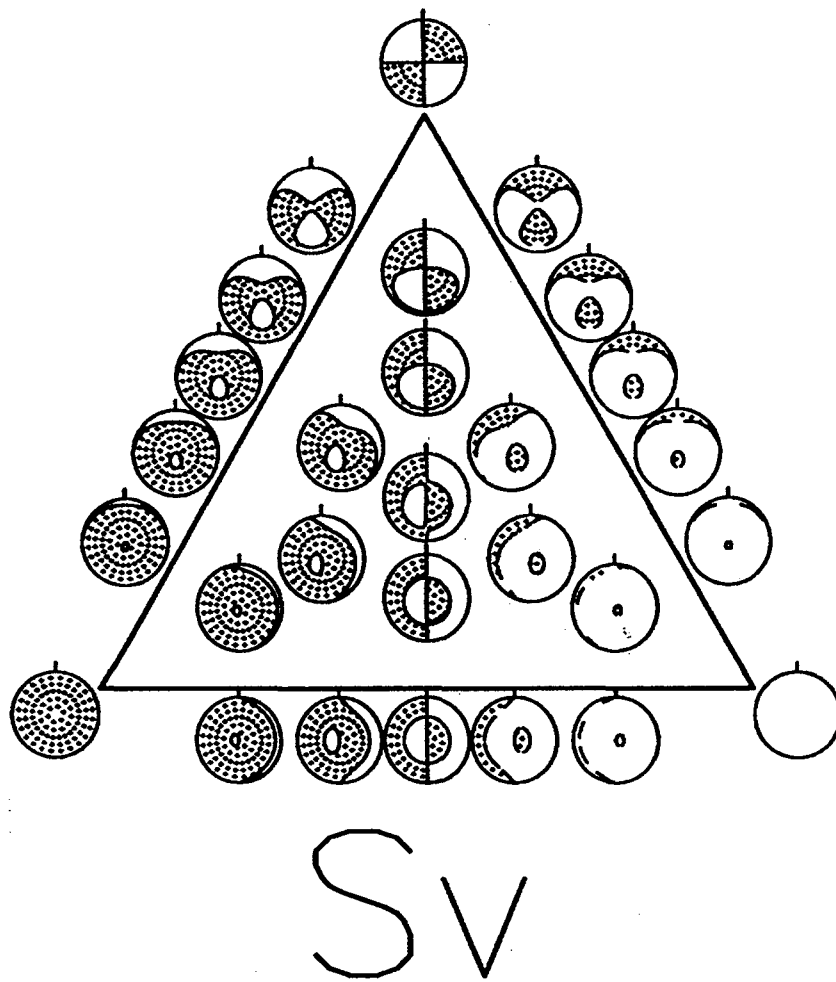


Figure 9c

$$\sin^2 \alpha_T + \sin^2 \alpha_B + \sin^2 \alpha_P = 1 \quad (40)$$

If we define $x = \sin \alpha_T$, $y = \sin \alpha_B$, and $z = \sin \alpha_P$, then eq. (40) is just the equation of the sphere $x^2 + y^2 + z^2 = 1$. Since all the angles are between 0° and 90° , plotting focal mechanisms on a triangle diagram is equivalent to the cartographer's problem of projecting locations from a quarter-hemisphere onto a triangular flat surface.

The map projection which does this is the azimuthal gnomonic projection. If χ is the angle defined by:

$$\chi = \tan^{-1}(\sin \alpha_T / \sin \alpha_P) - 45^\circ \quad (41)$$

then the horizontal position h and vertical positions v of a point on the triangle diagram are given by:

$$h = \frac{\cos \alpha_B \sin \chi}{\sin(35.26^\circ) \sin \alpha_B + \cos(35.25^\circ) \cos \alpha_B \cos \chi} \quad (42)$$

$$v = \frac{\cos(35.26^\circ) \sin \alpha_B - \sin(35.26^\circ) \cos \alpha_B \cos \chi}{\sin(35.26^\circ) \sin \alpha_B + \cos(35.26^\circ) \cos \alpha_B \cos \chi} \quad (43)$$

Here, 35.26° is the dip angle of the T , B , and P axes for the focal mechanism which plots in the exact center of the triangle diagram, where $h = v = 0$. Note that eqs. (42) and (43) are identical to the incorrect expressions which appear in Frohlich (1992) and Frohlich and Apperson (1992) except for the $\cos \alpha_B$ in the second term in the denominator.

Eq. (40) also provides a way of defining the fractional proportions of thrust, strike-slip, and normal faulting for any particular focal mechanism. In particular, if we define:

$$f_{\text{thrust}} = \sin^2 \alpha_T; f_{\text{strike-slip}} = \sin^2 \alpha_B; f_{\text{normal}} = \sin^2 \alpha_P \quad (44)$$

then eq. (40) is just $f_{\text{thrust}} + f_{\text{strike-slip}} + f_{\text{normal}} = 1$. Thus, for example, when the B axis is vertical $f_{\text{strike-slip}} = 1$ and f_{thrust} and f_{normal} are zero.

However, for a mechanism where all three dip angles are the same, equaling 35.26° , then $f_{\text{strike-slip}} = f_{\text{thrust}} = f_{\text{normal}} = 0.33$.

ACKNOWLEDGMENTS

Support for this work was provided by the Air Force Office of Scientific Research (Contracts F19628-91-K-0026, F49620-94-0287 and Phillips Laboratory Task 2309G2).

REFERENCES

- Barker, J. S. *A Seismological Analysis of the May 1980 Mammoth Lakes, California, Earthquakes*, Ph. D. thesis, Pennsylvania State University, 279 p., 1984.
- Frohlich, C. Cliff's nodes concerning plotting nodal lines for P, S_h and S_v , *Seismol. Res. Lett.*, 67, 16-24, 1996.
- Frohlich, C. Triangle diagrams: Ternary graphs to display similarity and diversity of earthquake focal mechanisms, *Phys. Earth Planet. Int.*, 75, 193-198, 1992.
- Frohlich, C. and K. D. Apperson. Earthquake focal mechanisms, moment tensors, and the consistency of seismic activity near plate boundaries, *Tectonics*, 11, 279-296, 1992.
- Julian, B. R. and G. R. Foulger. Identifying non-double-couple earthquakes by inverting seismic-wave amplitude ratios, *EOS*, 75 (44), 460, 1994.
- Kennett, B. L. N., Radiation from a moment-tensor source, in, *Seismological Algorithms: Computational Methods and Computer Programs*, ed. by D. D. Doornbos, pp. 427-441, Academic Press, London, 1988.
- Lay, T. and D. V. Helmberger. A lower mantle S-wave triplication and the shear velocity structure of D", *Geophys. J. Roy. Astr. Soc.*, 75, 799-838, 1983.

Pujol, J. and R. B. Herrmann. A student's guide to point sources in homogeneous media, *Seismol. Res. Lett.*, 61, 209-224, 1990.

Table 1: Principal moments and orientations of T , B , and P axes for all mechanisms plotted in this report.

	T axis			B axis			P axis		
	λ_T	φ_T	α_T	λ_B	φ_B	α_B	λ_P	φ_P	α_P
Fig. 1	1.57	120°	24°	0.27	8°	40°	-1.84	232°	41°
Fig. 2	2.00	90°	0°	+0.90	0°	90°	+0.10	0°	0°
	1.70	90°	0°	+0.60	0°	90°	-0.20	0°	0°
	1.00	90°	0°	-0.10	0°	90°	-0.90	0°	0°
	1.00	90°	0°	0.00	0°	90°	-1.00	0°	0°
	1.00	90°	0°	0.00	0°	90°	-0.10	0°	0°
Fig. 3	1.00	0°	0°	-0.50	90°	0°	-0.5	90°	90°
	1.00	0°	45°	-0.50	90°	0°	-0.5	180°	45°
	1.00	0°	90°	-0.50	90°	0°	-0.5	0°	0°
	1.00	90°	45°	-0.50	270°	45°	-0.5	0°	0°
	1.00	90°	0°	-0.50	90°	90°	-0.5	0°	0°
Fig. 4	0.50	236°	39°	-1.25	0°	35°	-2.25	116°	32°
	1.50	236°	39°	-0.25	0°	35°	-1.25	116°	32°
	1.50	265°	50°	-0.25	0°	4°	-1.25	93°	40°
	1.50	270°	50°	-0.25	180°	0°	-1.25	90°	40°
	1.50	180°	0°	-0.25	270°	50°	-1.25	90°	40°
Fig. 6	1.00	90°	0°	0.00	180°	90°	-1.00	0°	0°
	1.00	90°	0°	-0.40	180°	90°	-0.60	0°	0°
	1.00	270°	45°	0.00	180°	0°	-1.00	90°	45°
	1.00	0°	35.26°	0.00	120°	35.26°	-1.00	240°	35.26°
	1.00	0°	35.26°	-0.05	120°	35.26°	-0.95	240°	35.26°

To Obtain Cliff's Nodes Software From IRIS:

We assume that you are logged into a workstation with a UNIX operating system and connected to the Internet.

1. To connect to IRIS computer using file transfer program type:

```
ftp iris.washington.edu
```

Computer will ask for name and password; name is "anonymous" and password is your name, e. g., I type:

```
anonymous
```

```
cliff
```

2. Change directories on IRIS computer to subdirectories containing CliffsNodes software-- type:

```
cd pub
```

```
cd programs
```

```
cd sel
```

```
cd sun
```

3. Transfer the documentation and software to your computer-- type:

```
mget CliffsNodes*
```

The system will ask you specifically if you want to obtain files CliffsNodes.PShSv.README, and CliffsNodes.PShSv.tar. In each case you type:

```
y
```

Then, to leave the ftp program, type:

```
quit
```

4. To translate the tar file and create two subdirectories containing the software and the documentation, /cliff and /doc, type:

```
tar -xvf CliffsNodes.PShSv.tar
```

The computer will list all the files as it creates them.

5. To run the CliffsNodes demonstration program, type:

```
cd cliff
```

```
Node.demo
```